

Mesoporous Carbon for Supercapacitors



Hongzhen He, Yiyang Liu, Paul R. Shearing, Guanjie He,
and Dan J. L. Brett

Abstract With the further advancement of electrification, supercapacitors (SCs) have garnered numerous attention as promising electrochemical energy storage (EES) devices, due to their favourable characteristics such as, high energy density, ultrahigh power density and long cycling stability. To fully exploit their potential as a platform for efficient energy storage devices, it is critical to gain a more in-depth understanding of the relationship between electrochemical performance and materials. Mesoporous carbon has aroused considerable interests as potential material for energy-related applications results from its large surface area, fast mass/charge transfer kinetics, and high abundance of active sites. In this chapter, we first provide a basic understanding of the classification of supercapacitors and the corresponding working principles. Then, the mainstream synthetic route of mesoporous carbon will be introduced, including templating and template-free methods. Next, an in-depth discussion of the representative mesoporous carbon for SCs is provided. Finally, insights into the major challenges and effective strategies for future developments are summarized.

Keywords Supercapacitors · Fundamental theories · Mesoporous carbon · Material synthesis · Electrode materials

H. He and Y. Liu: Authors have equal contributions.

H. He · Y. Liu · P. R. Shearing · G. He (✉) · D. J. L. Brett
Electrochemical Innovation Lab (EIL), Department of Chemical Engineering, University College London (UCL), London WC1 7JE, UK
e-mail: g.he@ucl.ac.uk

D. J. L. Brett
e-mail: d.brett@ucl.ac.uk

G. He
School of Chemistry, University of Lincoln, Brayford Pool, Lincoln LN6 7TS, UK

P. R. Shearing · D. J. L. Brett
The Faraday Institution, Quad One, Becquerel Avenue, Harwell Campus, Didcot OX11 0RA, UK

1 Introduction

As energy demands continue to grow, traditional energy sources, such as petroleum, natural gas and coal, are harder to meet human's ambition for carbon neutrality and net-zero emission. Therefore, efficient energy conversion and storage has become a grand challenge to society. Researchers and enterprises currently focus their efforts on developing new electrochemical energy storage (EES) devices, including secondary batteries, fuel cells, and supercapacitors (SCs). Secondary EES devices represented by Li-ion batteries (LIBs) generally have a high energy density ($180 \sim 340 \text{ Wh kg}^{-1}$) and long durability, which dominates the EES market. However, their low power density ($100 \sim 300 \text{ W kg}^{-1}$), high cost ($\140 per kWh), limited raw material reserves and safety issues hindered their further development.

Although traditional capacitors could satisfy the high-power density demands, their low specific capacitance ($\leq 2.7 \text{ F g}^{-1}$) and energy density ($0.01 \sim 0.3 \text{ Wh kg}^{-1}$) retards the further deployments. Supercapacitors (SCs) are the devices that possess ultrahigh power density ($5 \sim 30 \text{ kW/kg}$), high energy conversion efficiency and long cycling durability ($>100,000$ cycles), which have become one of the most promising EES devices for high-power applications [4]. The electrochemical performance and characteristics of SCs sit between batteries and conventional capacitors; therefore, they have a much higher energy density (28 Wh kg^{-1}) than conventional capacitors. As illustrated in Fig. 1, it can be used as a starting source for vehicles and a power balance source for lifting devices. Additionally, it can be used as a source of traction energy for hybrid cars, internal combustion engines, trackless vehicles, and other equipment. Up to now, a wide range of materials have been reported as the electrodes

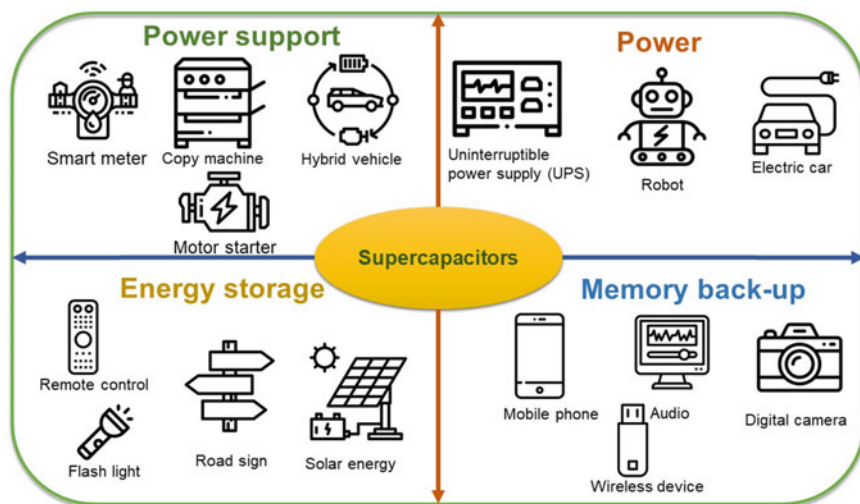


Fig. 1 Applications of supercapacitors

for SCs, such as carbon materials, covalent organic backbones (COFs), metal–organic backbones (MOFs), conductive polymers, transition metal compounds [20].

Mesoporous carbon materials have been widely investigated and used in many fields, including adsorption, separation, catalysis and EES applications. Mesoporous carbon materials are distinguished from conventional carbon materials by their controlled and superior properties in terms of synthetic routes, tunable pore structures and surface area. Compared to macroporous (> 50 nm) and microporous (< 2 nm) carbon, the mesoporous (2 ~ 50 nm) carbon possess a more suitable pore size for application in SCs: the macroporous carbon can not provide a high specific surface area; while the micropores are hard for electrolyte penetration and diffusion. Despite the excellent performance offered by mesoporous carbon in energy-oriented applications, there are several challenges for their practical application in SCs. Firstly, it is challenging to achieve mass-production for mesoporous carbon. Secondly, scalable synthetic solutions with optimised structural and compositional parameters remain critical. Until now, very few control methods for mesoporous carbon synthesis have been reported, particularly for spherical materials with tunable pore size and hydrophilicity. Thirdly, modification of the surface of mesoporous carbon remains challenging.

To provide an informative and inspiring understanding for researchers in the mesoporous carbon and SC-related fields, this Chapter will provide an informative introduction and discussion covering: (a) the working mechanisms of SCs (Sect. 2); (b) synthesis route of mesoporous carbon (Sect. 3); (c) representative mesoporous carbon electrodes for SCs (Sect. 4); (d) conclusion and perspectives (Sect. 5).

2 Working Principle of SCs

The earliest capacitors date back to the invention of the ‘Leiden’ bottle by Prof. Pieter Van Musschenbroek at Leiden University in the Netherlands in 1746. A typical Leiden bottle is a glass container covered inside and outside with conductive metal foil to act as a pole plate. The bottle’s top end is connected to a circular electrode, while the bottom end is connected to the inner metal foil or water via a conductor (usually a metal locking chain). A vintage ‘Layden bottle’ can achieve a high voltage of 20 ~ 60 kV and a low specific capacitance of ~ 1 nF (per pint of volume).

In 1853, the German physicist Helmholtz proposed a theoretical model of an interfacial double layer: under the action of a certain voltage, the interface between the electrode material and the electrolyte solution generates two layers of charges of the same quantity and opposite charges, thus forming a double layer. In 1957, Becker from General Motors prepared a small capacitor with porous carbon electrodes based on the double layer capacitance theory mentioned above, and named it a “supercapacitor”, which was first developed and brought to market by SOHIO in 1969. The technology was subsequently transferred to NEC Japan and commercialised as an aqueous high-capacitance capacitor in battery starting systems for electric vehicles.

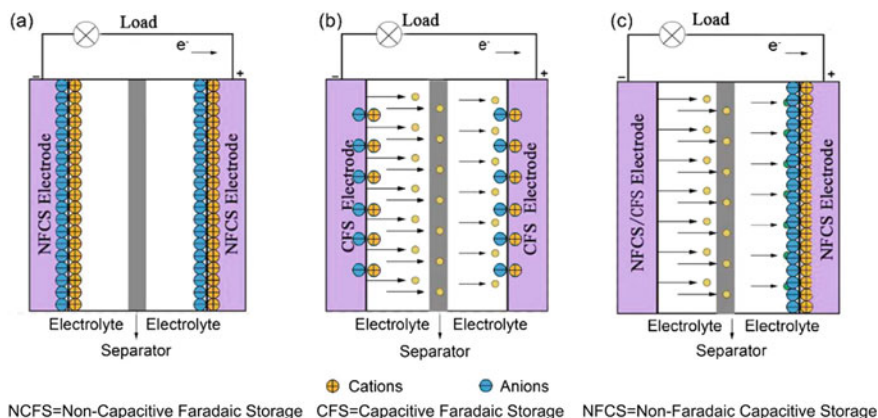


Fig. 2 Schematic illustration of **a** EDLC, **b** pseudocapacitor, and **c** Hybrid SC

Since then, SCs have attracted the attention of many countries, and comprehensive research has been carried out. In 1971, Sergio Trasatti and others discovered the outstanding capacitive properties of RuO_2 , which led to a boom in the development of pseudocapacitors based on metal oxide electrodes. After 1975, Brian E. Conway carried out RuO_2 -related research and commercial development attempts. Since then, pseudocapacitors with RuO_2 electrodes have been used in military applications. A wide range of inexpensive transition metal (hydro)oxides, heteroatom-doped carbon, conductive polymers, covalent organic frameworks (COFs) and other materials have been extensively investigated since the 1990s. As shown in Fig. 2, SCs consist of cathodes, anodes, electrolytes and separators. SCs could be classified as three types depending on the charge and energy storage mechanisms: electric double-layer capacitors (EDLCs), pseudocapacitors, and hybrid SCs.

2.1 EDLCs

The working principle of an EDLC is shown in Fig. 2a. Under the action of an electric field, an equal number of anions and cations in the electrolyte move towards the cathodes and anodes, respectively; this will create an electric potential difference and an EDL between the electrode and the electrolyte. After the removal of this electric field, the layers and voltage can be stabilized due to the anisotropic attraction of the charges. After connecting EDLC to the external circuit, the charged ions adsorbed on the two electrodes will move directionally until the electrolyte becomes electrically neutral again.

The relationship among total capacitor capacitance is C_T and capacitance of both electrodes (C_1 and C_2) can be expressed by the formula:

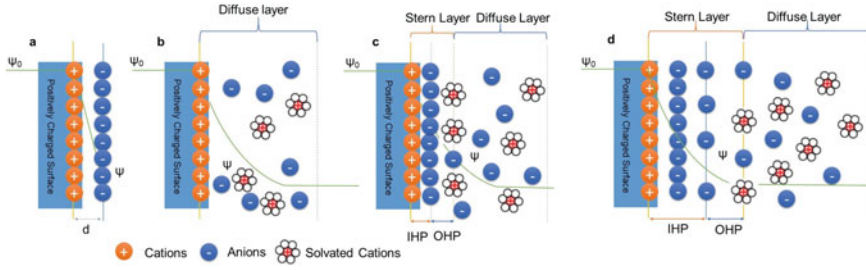


Fig. 3 Schematic diagram of EDL models. **a** Helmholtz model; **b** Gouy-Chapman (G-C) model; **c** Gouy-Chapman-Stern (G-C-S) model; **d** modified G-C-S model

$$\frac{1}{C_T} = \frac{1}{C_1} + \frac{1}{C_2} \quad (1)$$

Since 1853, numerous theories and models have been developed, the most notable ones include Helmholtz model, Gouy-Chapman (G-C) model, and Gouy-Chapman-Stern (G-C-S) model. The central concept of the Helmholtz model's is that opposite charges are distributed equally on both sides of the interface; additionally, this structure can be compared to a flat capacitor (Fig. 3a). Thus, Eq. (2) can be used to determine the unilateral charge density ($C \cdot m^{-3}$):

$$C = \frac{\varepsilon_r \varepsilon_0}{d} A \quad (2)$$

where C is the capacitance value, ε_r and ε_0 are the vacuum dielectric constant and the electrolyte dielectric constant, respectively; d is the effective thickness of the EDL; A is the specific surface area of the electrode material. Then, the capacitor capacitance (C_d) can be determined by:

$$C_d = \frac{\partial \sigma}{\partial V} = \frac{\varepsilon_r \varepsilon_0}{d} \quad (3)$$

It should be noted that C_d is a fixed value in the three formulas; however, C_d is actually affected by a series of factors, including relative potential, concentration of electrolyte, etc. Therefore, incorporating a diffuse layer model, The G-C model (Fig. 3b) was proposed. When the potential difference between two sides of the interface is large, more ions are compressed near the electrode; however, when the electrolyte concentration is high, the ions can also achieve charge equilibrium with the electrodes in a small space. In the G-C model, Helmholtz model's effective thickness (d) is converted into a variable, thereby allowing for a more accurate interpretation of the trend of C_d . Nevertheless, the C_d prediction in G-C model has several major shortcomings: (a) at both ends of the curve, C_d approaches infinity and contradicts actual tests; (b) could be significantly higher than the measured value; (c) low accuracy for capacitors with highly charged DLs. These deviations are inevitable since the

charges in G-C model are regarded as the mass points, which will be infinitely close to the surface of the electrodes under a large potential difference. Therefore, the distance between positive and negative charges will approach zero, which lead to a C_d approaching infinity [23].

Later on, based on G-C models, Otto Stern take ion size into condieration, and proposed the G-C-S model (Fig. 3c). At the electrode–electrolyte interface, the G-C-S model predicts two ion distribution regions: Helmholtz layer and Gouy-Chapman diffusion layer. The entire double-layer (C_{dl}) can be determined by capacitance generated in the diffusion layer (C_{diff}) and stern layer (C_H):

$$\frac{1}{C_{dl}} = \frac{1}{C_H} + \frac{1}{C_{diff}} \quad (4)$$

C_{dl} is always less than C_H and C_{diff} , according to Eq. (4). When the potential difference is small, C_{diff} has a negligible effect on C_{dl} and has a V-shaped curve versus potential difference; when the potential difference is large, C_{diff} has a large value and thus has a negligible effect on C_{dl} . The value of C_{dl} approaches C_H in this case. Nevertheless, there are serval drawbacks of the the G-C-S model: (a) the ions in the electrolyte will be surrounded by solvent ions, forming solvated ions; and (b) if the adsorption force at the interface exceeds the electrostatic force, even ions with similar charges will be stable at the interface.

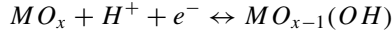
David C. Grahame proposed a modification to the G-C-S model in 1947, arguing that certain ions or uncharged substances could penetrate the Stern layer. When approaching the electrode in the modified G-C-S model, the term “specifically absorbed ions” refers to the ions losing their solvation shell and coming into direct contact with the electrode. As illustrated in Fig. 3d, the modified model predicted the presence of three regions: the inner Helmholtz plane (IHP), the outer Helmholtz plane (OHP), and the diffuse layer. The IHP denotes the distance between specifically absorbed ions and the OHP denotes the distance between non-specifically absorbed ions [3]. Despite the increasing precision and sophistication of these theories and models, the debate and further exploration still exist.

2.2 Pseudocapacitors

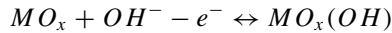
The charge and energy storage mechanism of pseudocapacitors relies on the underpotential deposition on the surface or in the bulk phase of electrode materials with electrochemical activity in two or quasi-two dimensions. This results in highly reversible chemisorption or redox reaction that generates a capacitance related to the electrode charging potential. The voltage of this electrode system varies linearly with the amount of charge transferred and exhibits a capacitive characteristic, hence the term “pseudocapacitor”, as a complementary form of EDLCs. Although they are not electrostatic in nature, they exhibit similar electrochemical properties to EDLC, such as cyclic voltammetry and charge/discharge curves. In general, pseudocapacitors tend

to have superior specific capacitance than traditional EDLCs. Nevertheless, with the occurrence of redox reactions during the cycling, the bulk phase of the active materials or the electrolyte composition is altered, which deteriorate the electrochemical stability of pseudocapacitors [5, 15, 18]. Take metal oxides as an example, the charging and discharging reaction process in an aqueous electrolyte is as follows:

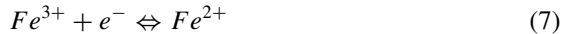
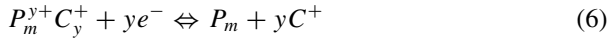
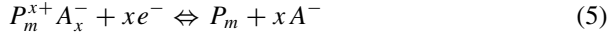
When the electrolyte is acidic:



When the electrolyte is alkaline:



Alternatively, the pseudo-capacitance effect can be increased by adding ions with redox activities to the electrolyte [6]. Ren et al. reported a pseudocapacitor using a porous nanoflower polyaniline (PANI) electrode and redox-active electrolyte (1 M H_2SO_4 + 0.8 M Fe^{2+}/Fe^{3+}), which demonstrates a high specific capacitance of 1062 $F\ g^{-1}$ ($2\ A\ g^{-1}$) and remarkable capacitance retention of 93% at 5 $A\ g^{-1}$ over 10,000 cycles (Ren et al. 2017). There are two redox systems in the as-assembled SC: (a) as shown in Eqs. (5) and (6), the conjugated double bonds in the PANI networks (P_m , m is the polymerization degree); (b) as shown in Eq. (7), the active Fe^{2+}/Fe^{3+} redox couples.



2.3 Hybrid SCs

The hybrid SCs combine the electrodes with different charge and energy storage mechanisms (Faradaic, capacitive, and capacitive-Faradaic processes), and increase the device energy density to 15–30 $Wh\ kg^{-1}$. The design of the components determines whether hybrid SCs are symmetrical or asymmetrical. When two separate electrodes comprised of different materials are combined in a hybrid supercapacitor, it exhibits better electrochemical behaviour than single electrodes. The hybrid technology preserves the level of cycle stability and affordability that has been a limiting factor in pseudocapacitor. The symmetric hybrid supercapacitor is made up of two same SC electrodes; while the asymmetric hybrid SC is made up of two different electrodes.

3 Synthesis of Representative Mesoporous Carbon

Numerous synthetic methodologies have been proposed, making it possible to prepare mesoporous carbon with various structures and morphologies. These methodologies could be classified as two categories: templating and template-free methods.

3.1 Templating Method

The templating method is the most widely studied methodology to prepare mesoporous carbon. Generally, the direct carbonisation of precursors is challenging to form mesoporous carbon with high surface area, which leads to limited electrochemical performance. In the templating methods, carbon is deposited on the surface of the template, thus forming a composite material, which can effectively generate carbon materials with desired structures and morphologies after removing the templates. In general, the templating method could be further classified as three types: hard templating, soft templating and hybrid templating.

3.1.1 Hard-Templating Method

Insoluble Templates

Although many metal/non-metal oxide and salt templates (*e.g.*, Al_2O_3 , ZnO , MgO , and SiO_2) are insoluble in water, they could be removed under specific solutions. With a high melting point and exceptional thermal/chemical/mechanical stability, oxide and insoluble salt templates preserve their original structures and morphologies at elevated temperatures. As a result, the space occupied by the template is retained following its removal. Simultaneously, the morphology and structure of the resultant carbon substance are opposed to those of the templates. For instance, Seo and colleagues synthesised a mesoporous carbon using furfuryl alcohol (FA) and acidified mesoporous silica impregnated with phosphoric or sulphuric acid as precursors. This work avoided the formation of undesired carbon by using a weak acid to catalyze and slow down the FA polymerisation [10].

Soluble Templates

In contrast to insoluble templates, soluble templates can be removed directly with water, thus avoiding harmful reagents. In addition, soluble templates could be recycled during the synthesis process. De-templated wastewater could be processed to a suitably concentrated template solution that can be re-involved in the synthesis.

Lee's group prepared a mesoporous carbon with uniform pores (~10 nm) by using a mesoporous aluminosilicate foam template and in situ polymerisation of phenolic resin. Strong acid catalytic sites for the polymerisation of phenol and formaldehyde are created by impregnating aluminium into the silicate backbone. Several different mesoporous aluminium silicate foams with different cell and window sizes have been synthesised as templates for many other mesoporous carbon foams. For example, using aluminium silicate foams with 30 nm cells and 14 nm windows as a template, a mesoporous carbon foam was obtained. The mesoporous carbon foam possess an even mesopore size of approximately 3.5 nm, which was achieved by removing the aluminosilicate template [7].

Ice Templating Method

Distinct from other hard templating methods, the ice template will be removed before the carbonisation of the precursors. The ice template indirectly influences the carbon material structures via altering the structure and composition of the carbon precursor, whereas the other hard templates directly influence the carbon material structure. In general, a typical ice templating comprises three phases. Firstly, the aqueous carbon precursors are swiftly frozen and crystallised in the first stage, where water condenses into ice over time. The second phase involves sublimating the ice crystals directly into water vapour by freeze-drying, resulting in a loose and porous structure. Carbonisation of the freeze-dried carbon precursors is the third phase. Although ice templates can significantly increase the surface area, it is challenging to regulate the shape and size of the ice crystals at the nanoscale. Therefore, additional procedures, typical activation or porogenic agents, are required to control the nanostructure of carbon aerogels.

3.1.2 Soft Templating Method

Soft templates are usually the amphiphilic molecules that can form micelles by the self-assembly process. Then, the micelles could be disintegrated at high temperatures, thus forming pores in the space they occupy. Soft-templating has been widely used to synthesise various mesoporous materials, including zeolites, silica, inorganic metal oxides, and mesoporous carbons. To successfully synthesise the mesoporous carbon precursor by the soft template method, the following three requirements must be met: (a) can form nanostructures by self-assembly; (b) consists of at least one component that can stably form pores at high temperatures; (c) consists of at least one kind of carbon-producing components. Currently, only a few materials meet these requirements. Moriguchi et al. successfully synthesised an ordered mesoporous carbon, through the ageing of the intermediate phase assembled by phenolic resin and cetyltrimethylammonium bromide (CTAB) as a template. The lamellar, hexagonal, and disordered intermediate phases were synthesised by varying the ratio of phenol to CTAB from 1:1 to 6:1 [16]. Li's group has also investigated the use

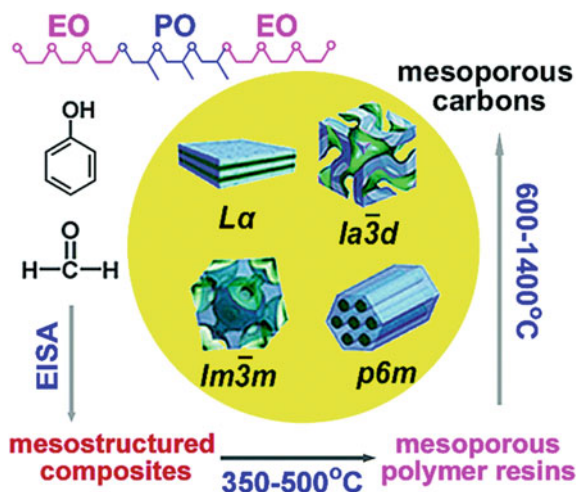
of CTAB as a soft template for the synthesis of mesoporous carbon [9]. The carbon precursor they used was a solubilized pitch material with negatively charged terminal groups; this micelle-templating strategy resulted in forming carbon materials with a vesicular and hierarchical structure. Zhao et al. also reported another method to synthesise mesoporous carbon materials using alkyl chain-based (Brij) surfactants. Although highly ordered mesophases were obtained, the carbonised materials lacked mesoporous structures. This is because the residual carbon from surfactants used can occupy the mesopore-generating spaces. Therefore, it is recommended to remove the surfactant molecules prior to carbonization via solvent extraction [14].

3.2 Template-Free Method

3.2.1 Pyrolysis Route

The traditional mesoporous carbon synthesis route (*e.g.*, chemical vapour deposition and arc discharge) are generally cumbersome and expensive, limiting their practical applications. However, the rapid pyrolysis of biomass into functionalised mesoporous carbon via thermochemistry is an environmentally friendly approach without air pollution generated from open burning. Therefore, Yu et al. proposed a scalable “green” method (Fig. 4) for the synthesis of nanofibers/mesoporous carbon composites via pyrolysis of Fe(iii)-preloaded biomass, which is controllable through temperature adjustment and the addition of the FeCl₃ catalyst. In an in situ CVD process, the combined catalytic action of Fe and Cl species were able to effectively catalyse the growth of carbon nanofibers on mesoporous carbon and the formation of magnetic nanofibers/mesoporous carbon composites. Additionally, the as-prepared

Fig. 4 Schematical illustration of mesoporous carbon materials synthesis using synthetic polymer precursor (Adapted with permission from Reference [14], Copyright (2006), ACS Publications)



material could be directly used as electrode materials for electrochemical energy storage without further separation and demonstrated a high specific capacitance of (128 F g^{-1} at 2 mV s^{-1}), remarkable cycling durability (98% capacitance retention over 10,000 cycles at 0.5 A g^{-1} [12].

3.2.2 Natural Biomass Precursors

Biomass is an ideal carbon precursor due to its porous structure, which simplifies the synthesis steps and reduces manufacturing costs. Also, the use of horticultural waste addresses solid waste management, lowers raw material costs, and addresses environmental concerns. Mesoporous carbon can be synthesised by high-temperature pyrolysis and physical/chemical activation of natural biomass. Currently, a variety of biomass precursors have been widely investigated, such as cellulose, chitin and lignin.

4 Mesoporous Carbon for Supercapacitors

4.1 Mesoporous Carbon (Pure Carbon)

Due to several favourable characteristics such as ease of synthesis, low cost and high electrical conductivity, activated carbon is widely used as the electrode material in EES devices. However, its low effective specific surface area hinders the practical deployment due to the presence of randomly connected micropores, which are difficult for electrolyte ions to access. To improve their performance, researchers have explored mesoporous carbon as electrodes for SCs. For example, mesoporous carbon synthesised by the carbonisation of a mixture of polyvinyl alcohol and inorganic salts exhibited a specific capacitance of 180 F g^{-1} at 100 mA cm^{-2} in H_2SO_4 [2]. The size and content of the mesopores will affect a wide range of electrochemical properties, including specific capacitance, energy/power density, and others. Wang et al. first prepared a mesoporous carbon nanofiber by restricting self-assembled triblock copolymers with soluble phenolic resins within the channels of anodic Al_2O_3 membranes. SEM and TEM observations revealed hexagonally arranged mesoporous channels coiled concentrically around the carbon nanofibers' longitudinal axis. The as-prepared high specific surface area ($>1424 \text{ m}^2 \text{ g}^{-1}$) carbon nanofiber was used as electrode materials in SCs with KOH and ethylene carbonate/diethyl carbonate (EC/DEC) electrolytes, which demonstrates constant value in the range of 152 F/g in sweep rates on 50 mV/s [19]. Pure mesoporous carbon generally possesses poor electrical conductivity and low capacitance, which cannot be used directly as SC electrodes. One effective strategy is to dope heteroatoms into mesoporous carbon, which will be discussed in the following parts.

4.2 *N-doped Mesoporous Carbon*

The presence of electron donor N in the mesoporous carbon can provide more active sites for fast redox reactions on the electrode surface, thus enhancing a variety of chemical/physical properties including wettability, electrical conductivity, surface affinity for electrolytes, etc. [10]. As illustrated in Fig. 4, Liu and colleagues proposed a template-catalyzed in situ polymerization and co-assembly method using urea formaldehyde (UF) as the precursor and the nitrogen source and polystyrene-block poly(acrylic acid) (PS-*b*-PAA) as a catalyst. The UF precursors can interact selectively with partially ionised poly(acrylic acid) segments via hydrogen bonding and electrostatic interactions, followed by in situ polymerisation of the UF resin/PS-*b*-PAA composite catalysed by acidic PAA chain segments. The resulting N-doped mesoporous carbon has a high N content of 19 wt%, a homogeneous and large pore size (9.5–17.2 nm), and a high surface area (458–476 m²g⁻¹). Owing to these favourable properties, the as-fabricated SC exhibits a high specific capacitance of 252 F g⁻¹ at 0.2 A g⁻¹ [13]. In addition, Wu et al. developed a facile synthetic route for the N-doped ordered nanoporous carbon (NONCs) based on the in situ coating of polydopamine on the surface of SBA-15 pores. The carbonisation of polydopamine/silica nanocomposites in N₂ followed by removal of the silica template resulted in the formation of NONC materials with a BET surface area of 1013 m²g⁻¹ [11]. However, the poor crystallinity of the material deteriorated its electrical conductivity. To solve this issue, Yuan et al. synthesised a graphite-nitride ordered mesoporous carbon (G-OMC) by using mesoporous NiO as the template/catalyst and dopamine as the precursor. G-OMC possesses a higher degree of graphitisation than those prepared with dopamine and pure SBA-15, mainly due to the catalytic graphitisation induced by the NiO additives [22] (Fig. 5).

4.3 *Other Non-Metal Doped Mesoporous Carbon Materials*

Incorporating both N and other dopants (*e.g.*, S, P, F and B) in the carbon framework is becoming increasingly popular in the carbon research community due to the synergistic effects of co-doped atoms. For each application, the appropriate combination of co-dopants should be carefully chosen. For instance, the swollen carbon interlayer produced by S doping facilitates the adsorption of larger electrolyte ions; the highly electronegative F functional group significantly enhances polarisation and refines the pore structure/surface; doping P into carbon can modulate the formation of various N configurations [17]. While some literature suggests that surface co-doping has beneficial synergistic effects on capacitive properties, the underlying mechanisms require further investigation.

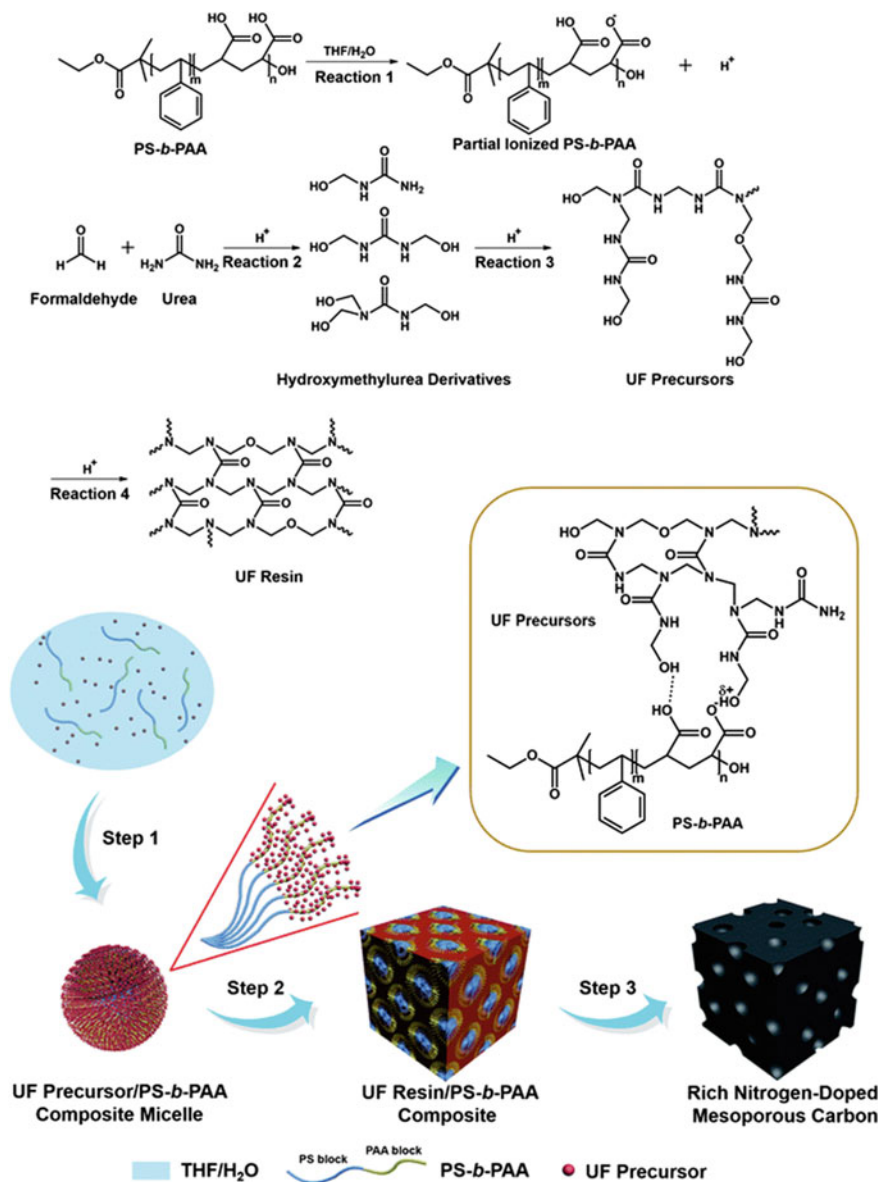


Fig. 5 The synthesis process of the abundant N-doped mesoporous carbon via in situ polymerization and co-assembly catalysed by a template (Adapted with permission from Reference [13], Copyright (2018), RSC Publications)

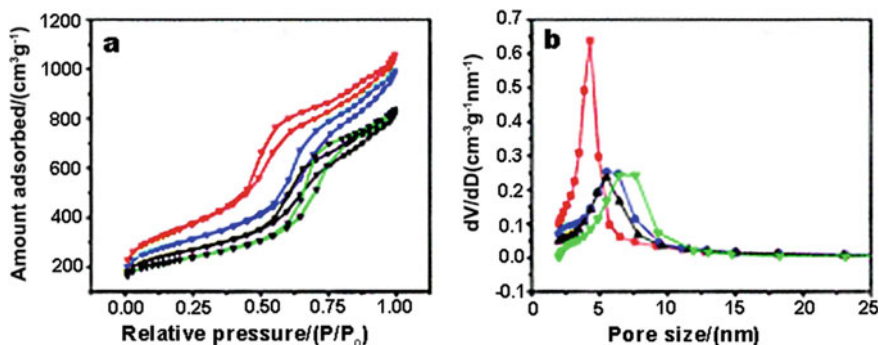


Fig. 6 **a** Nitrogen adsorption–desorption isotherms of ordered mesoporous carbon (OMC, red line), B-doped OMCs-1 (blue line), B-doped OMCs-2 (black line), and B-doped OMCs-3 (green line), **b** Pore size distributions of OMCs, B-doped OMCs-1, B-doped OMCs-2, and B-doped OMCs-3 (Adapted with permission from Reference [1], Copyright (2013), RSC Publications)

4.3.1 Boron-Doped Mesoporous Carbon

B doping will affect the electronic and electrical properties of the carbon nanostructures. As well as the thermal stability in the presence of nitrogen or air after substitution in the graphite skeleton. Coupling soft template and hydrothermal techniques, the evaporation-induced self-assembly (EISA) method using resorcinol and boric acid as precursors and Pluronic F127 as soft template was used to prepare B-OMC. However, the nitrogen adsorption data from three BOMCs in Fig. 6 demonstrate that the surface area and pore volume decrease as the B content increases. When B is incorporated into the OMC framework, micropores are lost, resulting in a decrease in the specific surface area and pore volume.

4.3.2 Phosphorus-Doped Mesoporous Carbon

Phosphorus is a member of the V group element in periodic table and shares the same number of valence electrons as nitrogen. Zhang's laboratory reported an ultra-convenient and energy-efficient microwave irradiation method for the fabrication of phosphorus-doped mesoporous carbon under ambient atmosphere. The prepared phosphorus-doped mesoporous carbon exhibits a high specific surface area (up to 2055 m²g⁻¹), a large pore volume (up to 2.73 cm³ g⁻¹) and good electrical conductivity. It also has a specific capacitance of up to 210 F g⁻¹, maintains a capacitance of over 201 F g⁻¹ even at high current densities of 20 A g⁻¹ and achieves a capacitance retention rate of 97.39% after 10,000 charge/discharge cycles. Comparative studies showed that similar morphologies were obtained by microwave irradiation and conventional pyrolytic carbonisation, but a more developed porosity and higher

degree of graphitisation was obtained under microwave irradiation. The carbonisation process under microwave irradiation is completed in 1–3 min, whereas conventional pyrolysis typically takes more than 2 h at temperatures above 600 °C. No rapid increase in surface oxygen content was observed, even when produced under ambient atmosphere. Such samples have the potential to become cost-effective and high-performance electrode materials for commercial SCs [8].

4.4 Hierarchical Porous Carbon (HPC)

When used as electrode materials in EES devices, HPCs exhibit a multimodal pore size distribution of micro-, meso-, and/or macropores, resulting in a high electrochemically accessible surface area and mass transfer rate. Typically, HPCs are prepared using templating techniques or a combination of templating and activation techniques. After combination and chemical activation, Xing's team synthesised a series of HPCs. The pore structure analysis revealed that micropores could be generated in a controlled manner within the mesoporous walls of the mesoporous carbon during the activation process. The prepared HPCs exhibit better capacitive properties than the hard template ordered mesoporous carbon, maintaining a high capacitance of 180 F g⁻¹ at high frequencies of 1 Hz. This can be attributed to the additional capacitance due to the generated micropores [21].

5 Conclusion and Perspective

SCs are promising EES devices to complement or even replace LIBs in various applications. This results from their favourable characteristics, including high power density, excellent cycle life, etc. This chapter presents and discusses the working principles, representative synthesis routes and optimisation of mesoporous carbon materials for SCs. Although many enlightening researches have been reported, more efforts are needed to bridge the large gap between laboratory-based research and commercial applications. Although these measurements are made using adsorption and theoretical models, the electrode pore structure is far more complex. Charge shielding, ion rearrangement, and sparse ionic pores will affect capacitance and ion dynamics. Therefore, more advanced characterization techniques such as micro/nano computerized tomography (CT) are recommended for further investigations. Also, future research could focus on improving carbon/electrolyte compatibility by adjusting micropore diameter/shape to accommodate larger electrolyte ions, adding meso/macropore pathways to transfer viscous media, and doping pseudo-active sites to improve interfacial interactions. For redox reactions and phase transitions, the improved device architecture must optimise carbon/electrolyte compatibility. Although challenges remain, we believe high-power, long-runtime

carbon-based supercapacitors will be developed soon for commercial applications in electronics and other fields.

Acknowledgements The authors would like to thank the Engineering and Physical Sciences Research Council (EPSRC, EP/533581/1), STFC Batteries Network (ST/R006873/1), RSC Mobility Grant (M19-7656) and Faraday Institution (EP/S003053/1) Degradation project (FIRG001) for financial support.

References

1. X. Bo, L. Guo, Ordered mesoporous boron-doped carbons as metal-free electrocatalysts for the oxygen reduction reaction in alkaline solution. *Phys. Chem. Chem. Phys.* **15**, 2459–2465 (2013). <https://doi.org/10.1039/c2cp43541a>
2. J.A. Fernández, T. Morishita, M. Toyoda, M. Inagaki, F. Stoeckli, T.A. Centeno, Performance of mesoporous carbons derived from poly(vinyl alcohol) in electrochemical capacitors. *J. Power Sources* **175**, 675–679 (2008). <https://doi.org/10.1016/j.jpowsour.2007.09.042>
3. D.C. Grahame, The electrical double layer and the theory of electrocapillarity. *Chem. Rev.* **41**, 441–501 (1947). <https://doi.org/10.1021/cr60130a002>
4. G. He, M. Ling, X. Han, D.I. Abou El Amaiem, Y. Shao, Y. Li, W. Li, S. Ji, B. Li, Y. Lu, R. Zou, F. Ryan Wang, D.J.L. Brett, Z. Xiao Guo, C. Blackman, I.P. Parkin, Self-standing electrodes with core-shell structures for high-performance supercapacitors. *Energy Storage Mater.* **9**, 119–125 (2017). <https://doi.org/10.1016/j.ensm.2017.07.005>
5. L. Hou, Y. Shi, C. Wu, Y. Zhang, Y. Ma, X. Sun, J. Sun, X. Zhang, C. Yuan, Monodisperse metallic NiCoSe₂ hollow sub-microspheres: formation process, intrinsic charge-storage mechanism, and appealing pseudocapacitance as highly conductive electrode for electrochemical supercapacitors. *Adv. Funct. Mater.* **28**, 1705921 (2018). <https://doi.org/10.1002/adfm.201705921>
6. R. Kushwaha, S. Haldar, P. Shekhar, A. Krishnan, J. Saha, P. Hui, C.P. Vinod, C. Subramaniam, R. Vaidhyanathan, Exceptional capacitance enhancement of a non-conducting COF through potential-driven chemical modulation by redox electrolyte. *Adv. Energy Mater.* **11**, 2003626 (2021). <https://doi.org/10.1002/aenm.202003626>
7. J. Lee, K. Sohn, T. Hyeon, Fabrication of novel mesocellular carbon foams with uniform ultralarge mesopores. *J. Am. Chem. Soc.* **123**, 5146–5147 (2001). <https://doi.org/10.1021/ja015510n>
8. Y. Li, D. Zhang, M. Han, J. He, Y. Wang, K. Wang, Y. Wang, Fabrication of the phosphorus doped mesoporous carbon with superior capacitive performance by microwave irradiation under ambient atmosphere: an ultra-facile and energy-efficient method. *Appl. Surf. Sci.* **458**, 119–128 (2018). <https://doi.org/10.1016/J.APSUSC.2018.07.089>
9. Z. Li, W. Yan, S. Dai, A novel vesicular carbon synthesized using amphiphilic carbonaceous material and micelle templating approach. *Carbon* **42**, 767–770 (2004). <https://doi.org/10.1016/j.carbon.2004.01.044>
10. H.W. Liang, W. Wei, Z.S. Wu, X. Feng, K. Müllen, Mesoporous metal-nitrogen-doped carbon electrocatalysts for highly efficient oxygen reduction reaction. *J. Am. Chem. Soc.* **135**, 16002–16005 (2013). <https://doi.org/10.1021/ja407552k>
11. Y. Liang, H. Liu, Z. Li, R. Fu, D. Wu, In situ polydopamine coating-directed synthesis of nitrogen-doped ordered nanoporous carbons with superior performance in supercapacitors. *J. Mater. Chem. A* **1**, 15207–15211 (2013). <https://doi.org/10.1039/c3ta13395h>
12. W.J. Liu, K. Tian, Y.R. He, H. Jiang, H.Q. Yu, High-yield harvest of nanofibers/mesoporous carbon composite by pyrolysis of waste biomass and its application for high durability electrochemical energy storage. *Environ. Sci. Technol.* **48**, 13951–13959 (2014). <https://doi.org/10.1021/es504184c>

13. Y. Liu, Z. Wang, W. Teng, H. Zhu, J. Wang, A.A. Elzatahry, D. Al-Dahyan, W. Li, Y. Deng, D. Zhao, A template-catalyzed: In situ polymerization and co-assembly strategy for rich nitrogen-doped mesoporous carbon. *J. Mater. Chem. A* **6**, 3162–3170 (2018). <https://doi.org/10.1039/c7ta10106f>
14. Y. Meng, D. Gu, F. Zhang, Y. Shi, L. Cheng, D. Feng, Z. Wu, Z. Chen, Y. Wan, A. Stein, D. Zhao, A family of highly ordered mesoporous polymer resin and carbon structures from organic-organic self-assembly. *Chem. Mater.* **18**, 4447–4464 (2006). <https://doi.org/10.1021/cm060921u>
15. Y. Meng, K. Wang, Y. Zhang, Z. Wei, Hierarchical porous graphene/polyaniline composite film with superior rate performance for flexible supercapacitors. *Adv. Mater.* **25**, 6985–6990 (2013). <https://doi.org/10.1002/adma.201303529>
16. I. Moriguchi, A. Ozono, K. Mikuriya, Y. Teraoka, S. Kagawa, M. Kodama, Micelle-templated mesophases of phenol-formaldehyde polymer. *Chem. Lett.* 1171–1172 (1999). <https://doi.org/10.1246/cl.1999.1171>
17. J.P. Paraknowitsch, A. Thomas, Doping carbons beyond nitrogen: an overview of advanced heteroatom doped carbons with boron, sulphur and phosphorus for energy applications. *Energy Environ. Sci.* **6**, 2839–2855 (2013). <https://doi.org/10.1039/c3ee41444b>
18. H. Tang, J. Wang, H. Yin, H. Zhao, D. Wang, Z. Tang, Growth of polypyrrole ultrathin films on mos2 monolayers as high-performance supercapacitor electrodes. *Adv. Mater.* **27**, 1117–1123 (2015). <https://doi.org/10.1002/adma.201404622>
19. K. Wang, Y. Wang, Y. Wang, E. Hosono, H. Zhou, Mesoporous carbon nanofibers for supercapacitor application. *J. Phys. Chem. C* **113**, 1093–1097 (2009). <https://doi.org/10.1021/jp807463u>
20. Z.-S. Wu, Y. Zheng, S. Zheng, S. Wang, C. Sun, K. Parvez, T. Ikeda, X. Bao, K. Müllen, X. Feng, Z. Wu, S.H. Zheng, S. Wang, C.L. Sun, X.H. Bao, Y.J. Zheng, K. Parvez, K. Müllen, X.L. Feng, Stacked-layer heterostructure films of 2D thiophene nanosheets and graphene for high-rate all-solid-state pseudocapacitors with enhanced volumetric capacitance. *Adv. Mater.* **29**, 1602960 (2017). <https://doi.org/10.1002/adma.201602960>
21. W. Xing, C.C. Huang, S.P. Zhuo, X. Yuan, G.Q. Wang, D. Hulicova-Jurcakova, Z.F. Yan, G.Q. Lu, Hierarchical porous carbons with high performance for supercapacitor electrodes. *Carbon* **47**, 1715–1722 (2009). <https://doi.org/10.1016/j.carbon.2009.02.024>
22. D. Yuan, F. Zeng, J. Yan, X. Yuan, X. Huang, W. Zou, A novel route for preparing graphitic ordered mesoporous carbon as electrochemical energy storage material. *RSC Adv.* **3**, 5570–5576 (2013). <https://doi.org/10.1039/c3ra40677f>
23. L. Zhang, X.S. Zhao, Carbon-based materials as supercapacitor electrodes. *Chem. Soc. Rev.* **38**, 2520–2531 (2009). <https://doi.org/10.1039/b813846j>